Available online at www.sciencedirect.com
SCIENCE DIRECT®
ELSEVIER
Microelectronics Reliability 44 (2004) 1033–1038
MICROELECTRONICS RELIABILITY
www.elsevier.com/locate/microrel

Degradation of AlGaN/GaN HEMTs under elevated temperature lifetesting

Y.C. Chou *, D. Leung, I. Smorchkova, M. Wojtowicz, R. Grundbacher, L. Callejo, Q. Kan, R. Lai, P.H. Liu, D. Eng, A. Oki

Northrop Grumman Space Technology, One Space Park, Redondo Beach, CA 90278, USA

Received 19 January 2004; received in revised form 16 February 2004
Available online 10 May 2004

Abstract

Elevated temperature lifetesting was performed on 0.25 μm AlGaN/GaN HEMTs grown by MOCVD on 2-in. SiC substrates. A temperature step stress (starting at T_a of 150 °C with a step of 15 °C; ending at T_a of 240 °C; 48 h for each temperature cycle) was employed for the quick reliability evaluation of AlGaN/GaN HEMTs. It was found that the degradation of AlGaN/GaN HEMTs was initiated at ambient temperature of 195 °C. The degradation characteristics consist of a decrease of drain current and transconductance, and an increase of channel-on-resistance. However, there is no noticeable degradation of the gate diode (ideality factor, barrier height, and reverse gate leakage current). The FIB/STEM technique was used to examine the degraded devices. There is no detectable ohmic metal or gate metal inter-diffusion into the epitaxial materials. Accordingly, the degradation mechanism of AlGaN/GaN HEMTs under elevated temperature lifetesting differs from that observed in GaAs and/or InP HEMTs. The reliability performance was also compared between two vendors of AlGaN/GaN epilayers. The results indicate that the reliability performance of AlGaN/GaN HEMTs could strongly depend on the material quality of AlGaN/GaN epitaxial layers on SiC substrates.
© 2004 Elsevier Ltd. All rights reserved.

1. Introduction

AlGaN/GaN HEMTs have demonstrated excellent power handling capability significantly outperforming state-of-the-art power performance of their counterparts—GaAs and InP based HEMTs. Continuous-wave (CW) power densities of AlGaN/GaN HEMTs as high as 11.2 W/mm have been demonstrated at 10 GHz [1]. AlGaN/GaN HEMT X-band power amplifiers achieved CW output power level up to 22.9 [2] and 38 W [3]. The superb power performance of AlGaN/GaN HEMTs is attributed to the combinations of high breakdown field (3×10^6 V/cm) due to large bandgap, high electron saturation (2×10^7 cm/s) and overshoot velocities (3×10^7 cm/s), and high electron sheet density (1×10^{13} cm^{-2}) [4]. The high electron sheet density is due to strong spontaneous and piezoelectric polarization without intentional doping in AlGaN–GaN heterostructure. Accordingly, AlGaN/GaN HEMTs could potentially become the critical components in the areas of satellite communications and high-performance radar applications.

To ensure the reliable operation of AlGaN/GaN HEMTs for high power amplifiers in a variety of military and space applications, it is essential to demonstrate high reliability performance for the potential insertion of AlGaN/GaN HEMTs. Recently, most reliability studies of AlGaN/GaN HEMTs were focused on hot electron stress either under high V_{ds} and/or RF overdrive at room temperature [5–8]. The primary degradation mechanism is attributed to the hot electrons generated in the region between the gate and drain under either high V_{ds} or high RF overdrive stress. The generated hot electrons are likely to be trapped in the interface between the

* Corresponding author.
E-mail address: yeong-chang.chou@ngc.com (Y.C. Chou).

0026-2714/$ - see front matter © 2004 Elsevier Ltd. All rights reserved.
doi:10.1016/j.microrel.2004.03.008

passivation layer and AlGaN barrier layer or in the AlGaN barrier layer. The trapped hot electrons could widen the surface depletion region, thus leading to the resultant DC and RF degradations [5]. Furthermore, Si_3N_4 passivation was found to be more resistant to the hot-carrier-induced-degradation (HCID) than SiO_2 passivation under DC and RF overdrive stress [6]. Nevertheless, the reliability investigation of AlGaN/GaN HEMTs under elevated temperature is still lacking. Although DC and RF overdrive stress of AlGaN/GaN HEMTs at room temperature provide reliability information owing to hot electron effect, it is important to explore the reliability of AlGaN/GaN HEMTs subjected to elevated temperature lifetesting in order to warrant the potential insertion of AlGaN/GaN HEMTs for the military and space applications.

In this paper, we investigate the degradation characteristics of AlGaN/GaN HEMTs under elevated temperature lifetesting. It has been found that the degradation mechanism of AlGaN/GaN HEMTs under elevated temperature lifetesting is different from that of GaAs and/or InP HEMTs. Furthermore, the reliability performance of AlGaN/GaN HEMTs between two epitaxial layer vendors was compared. It was found that the reliability performance of AlGaN/GaN HEMTs strongly depends on the material quality.

2. Device technology

The AlGaN/GaN HEMT structure was grown by metalorganic chemical vapor deposition (MOCVD) on 2-in. semi-insulating SiC substrates from vendor A. SiC substrates with a thermal conductivity of 4.9 W/cm K are known to provide better thermal management compared to sapphire substrates which have a thermal conductivity of 0.5 W/cm K. Accordingly, SiC was chosen as the base-line substrates for AlGaN/GaN epilayer growth in Northrop Grumman Space Technology (NGST). Fig. 1 shows the device structure used in this study, consisting of a 0.1-μm AlN nucleation layer, a 1-μm-thick GaN buffer layer, and a 250 Å $Al_{0.28}Ga_{0.72}N$ barrier layer. Owing to the large lattice mismatch between AlGaN/GaN and SiC substrates, an AlN nucleation layer was grown to prevent the misfit dislocations induced in SiC–AlN interface from propagating into GaN–AlGaN epilayers. A micrograph (shown in Fig. 2) of scanning-transmission-electron-microscopy (STEM) using a focused-ion-beam (FIB) technique to prepare the cross-section illustrates that misfit locations originated from AlN–SiC were confined in the AlN nucleation layer. However, there are still misfit locations originated from AlN–GaN and extending further into AlGaN epilayer.

The measured Hall sheet carrier concentration and electron mobility are 1.6×10^{13} cm^{-2} and 1146 cm^2/V s, respectively. The AlGaN/GaN HEMT fabrication process is based on NGST's mature GaAs and InP HEMTs technologies designed for high-volume production. The device mesa etch was performed using $BCl_3/Cl_2/Ar$ with inductively coupled plasma (ICP) etching technique. Ti/Al/Pt/Au metal stacks were annealed at 860 °C in a N_2 ambient to form the ohmic contacts with an average contact resistance of 0.65 Ω mm. A 0.25 μm T-gate with Pt/Au metal stacks was patterned by two layers (PMMA, P(MMA-MAA)) electron beam lithography followed by PECVD nitride passivation.The details were reported by Smorchkova et al. [9]. The fabricated AlGaN/GaN HEMTs demonstrate the maximum drain current density greater than 1 A/mm at $V_{gs} = +1$ V and the average peak transconductance greater than 250 mS/mm. The on-state V_{ds} burnout voltage at $I_{ds} = 500$ mA/mm is as high as 40 V. The cutoff frequency F_t and maximum oscillation frequency F_{max} at V_{ds} of 20 V and I_{ds} of 425 mA/mm are 44 and 80 GHz, respectively. The

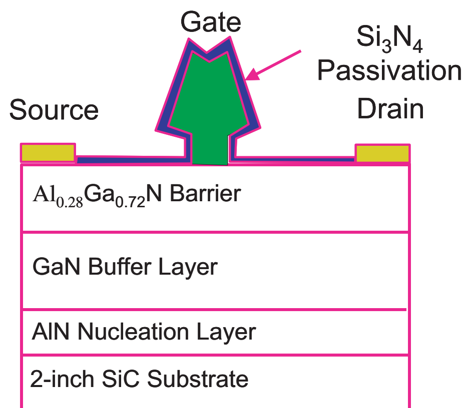

Fig. 1. Cross-section of an AlGaN/GaN HEMT.

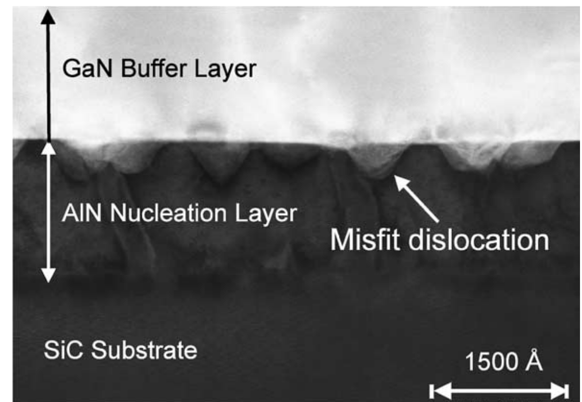

Fig. 2. A STEM micrograph showing the SiC substrate, AlN nucleation layer and GaN buffer layer.

excellent power and noise performance of AlGaN/GaN HEMTs at frequency of 20 GHz and beyond using NGST's AlGaN/GaN HEMT technology were described in Refs. [10–12].

3. Lifetest results and discussion

AlGaN/GaN HEMTs of sample size 10 with four gate fingers and 200 μm gate periphery were mounted on a 16-pin dual-in-line package (DIP) for elevated temperature lifetesting in N_2 ambient, starting from T_a of 150 °C and ending at T_a of 240 °C with a step of 15 °C and a 48 h cycle for each temperature. The devices were stressed at V_{ds} of 10 V and I_{ds} of 500 mA/mm with an estimate junction temperature rise of 150 °C based on finite-element thermal simulation. The comprehensive DC characteristics of forward/reverse diodes, I_{ds}–V_{gs} and I_{ds}–V_{ds} characteristics were measured on AlGaN/GaN HEMTs before and after lifetesting. Fig. 3 shows the I_{ds} degradation versus lifetesting ambient temperature. It was observed that device degradation was initiated approximately at ambient temperature of 195 °C. Fig. 4 illustrates that the degradation of I_{max} (measured at $V_{ds} = 5$ V and $V_g = +1$ V) and peak transconductance (G_{mp}) tracks the increase of channel-on-resistance (measured at linear region of I_{ds}–V_{ds} characteristics close to $V_{ds} = 0$ V). Since hot-carrier-induced-degradation has negative temperature coefficient, it is unlikely that the increase of channel-on-resistance observed in our stress conditions is due to the hot-electron trapping effect, typically incurred during the high V_{ds} and/or RF-overdrive stress at room temperature.

The I_{ds}–V_{ds} characteristics on a degraded AlGaN/GaN HEMT after lifetesting at T_a of 210 °C are shown in Fig. 5. Devices exhibit I_{ds} and G_m decreases. Fig. 6 shows a typical evolution of I_{ds}–V_{gs} characteristics of AlGaN/GaN HEMT under elevated temperature lifetesting. It was observed that the change of pinch-off voltage is negligible with a slight shift of V_g at peak G_{mp}. In addition, characteristics of gate-drain and gate-source diodes were examined. As shown in Fig. 7, only slight reduction of reverse gate current was observed. The degradation of forward diodes is unnoticeable. This information indicates that the area underneath the gate metal is probably not the origin of degraded AlGaN/GaN HEMTs under

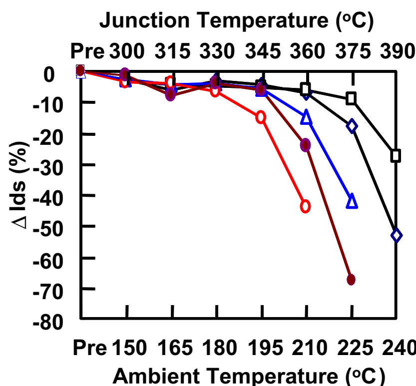

Fig. 3. ΔI_{ds} (measured at $V_{ds} = 5$ V and $V_g = 0$ V) versus lifetesting ambient temperature on AlGaN/GaN HEMTs grown by vendor A.

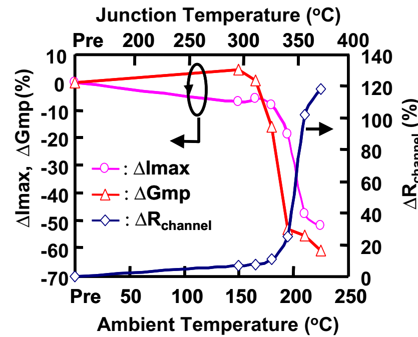

Fig. 4. Correlation of ΔI_{max}, ΔG_{mp}, and $\Delta R_{channel}$ versus lifetesting ambient temperature.

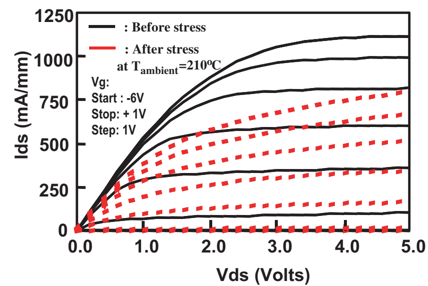

Fig. 5. I_{ds}–V_{ds} characteristics of a degraded AlGaN/GaN HEMT compared to those of a device before elevated temperature step stress.

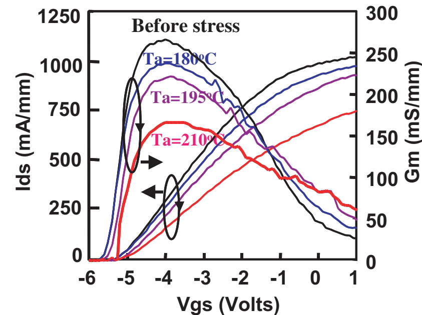

Fig. 6. The evolution of I_{ds}–V_{gs} characteristics of an AlGaN/GaN HEMT subjected to elevated temperature lifetesting.

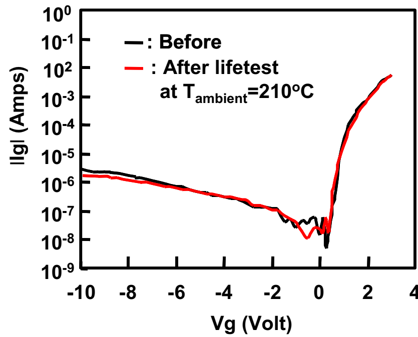

Fig. 7. Reverse and forward diode characteristics of an AlGaN/GaN HEMT before and after elevated temperature stress.

elevated temperature lifetesting because devices degradation induced by gate sinking exhibit Gm and pinch-off voltage shift as reported by Chou et al. [13].

Moreover, FIB, STEM, and high-resolution energy-dispersive-analysis with X-ray (EDX) were introduced to explore the physical evidence of a degraded AlGaN/GaN HEMTs. While conventional TEM has long been a standard tool for high-resolution imaging, the STEM has evolved rapidly into a nano-analytical tool while maintaining the atomic resolution imaging capability of TEM. An EDX tool with high-resolution capability is incorporated into the STEM for the chemical analysis if necessary. The combinations of FIB, STEM, and high-resolution EDX, in addition to electrical characterization, provide the powerful capability to resolve the degradation of AlGaN/GaN HEMTs induced by elevated temperature lifetesting.

This technique was also used for the degradation analysis in GaAs HEMTs under accelerated temperature lifetesting to disclose the complete phenomenon of gate-metal-sinking-induced-degradation (GSID) mechanism in GaAs HEMTs [13]. Fig. 8 shows a STEM micrograph on a degraded AlGaN/GaN HEMT after lifetesting at

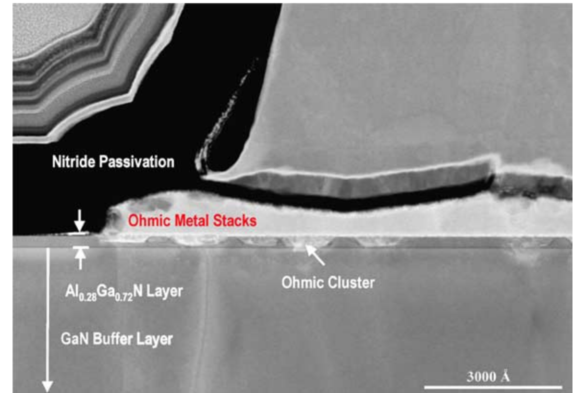

Fig. 9. Close view of a STEM micrograph on the ohmic region of a degraded AlGaN/GaN HEMT (as shown in Fig. 8).

ambient temperature of 240 °C, exhibiting more than 50% degradation of I_{max} and G_{mp}. A STEM on a virgin device was also performed as the control. It was observed that the misfit dislocations originate from the AlN–GaN interface and extend up to AlGaN layer on both virgin and degraded devices. It is still unclear if the misfit dislocations might cause the degradation in our lifetesting. The STEM close view of the ohmic metal region on a degraded device is shown in Fig. 9. There is no signature that ohmic metal interdiffusion is responsible for the degradation of AlGaN/GaN HEMTs. In addition, as shown in Fig. 9, ohmic clusters were formed during ohmic annealing at 860 °C in order to facilitate the ohmic contact formation. Ohmic clusters were observed on both virgin and degraded devices. Fig. 10 shows a STEM close view of the interface between gate metal and AlGaN barrier layer on a degraded sample, showing no evidence of gate metal interdiffusion involved in the degradation of AlGaN/GaN HEMTs induced by elevated temperature lifetesting.

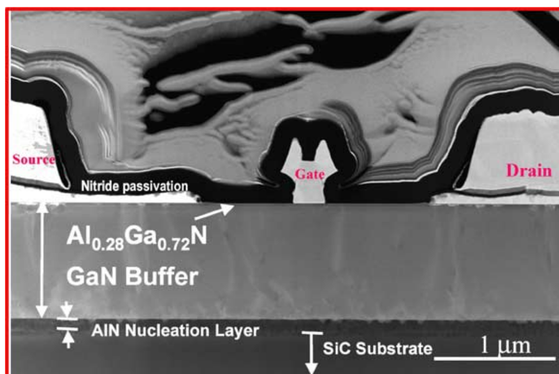

Fig. 8. A STEM micrograph of a degraded AlGaN/GaN HEMT after elevated temperature lifetesting at ambient temperature of 240 °C for 48 h.

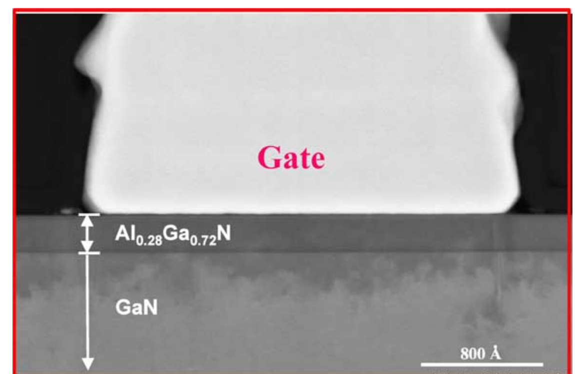

Fig. 10. High magnification of a STEM micrograph on a degraded AlGaN/GaN HEMT (as shown in Fig. 8). No signature of gate metal sinking was observed.

The STEM results from Figs. 9 and 10 further substantiate the DC evolution in Fig. 6. These are different from the results in GaAs HEMTs induced by elevated temperature lifetesting [14]. What might cause the observed degradation here is still not clear. We speculate that the degradation might be induced by the change of surface charge distribution between the nitride passivation and the AlGaN barrier layer, ohmic contact resistance degradation of Ti/Al/Pt/Au ohmic metal stacks or imperfect material quality (e.g., misfit dislocation in the epilayers) on AlGaN/GaN HEMTs subjected to elevated temperature lifetesting. The concrete degradation mechanism is still under investigation.

4. Dependence of reliability on material vendors

Similar lifetesting with sample size of 10 was also performed on AlGaN/GaN HEMTs fabricated onto the epitaxial layers from vendor B. As shown in Table 1, the devices from vendor B have reverse I_g of −78 μA at V_g of −10 V, which is much higher than the devices fabricated from vendor A with reverse I_g of −2.16 μA at V_g of −10 V, even though the devices from both vendors A and B demonstrate equivalent DC and RF characteristics. However, devices fabricated from vendor B exhibit significant degradation after lifetesting at ambient temperature of 150 °C for 48 h, while the degradation at this condition from vendor A's devices is negligible. This result suggests that the reliability performance of AlGaN/GaN HEMTs could strongly depend on the material quality among different vendors. The material quality could be affected by the variations of epilayer thickness, Al concentration in AlGaN layer, and defects in the epilayers. As shown in Fig. 8, the misfit dislocations originating from AlN–GaN interface could propagate into AlGaN barrier layer. Although misfit dislocations were believed to modify the local charge distribution, it is still unclear if the misfit dislocations might affect the reliability performance in AlGaN/GaN HEMTs. Based on the reliability performance dependence on different vendors, the improvement of material quality of AlGaN/GaN HEMT heterostructure on SiC substrate plays an important role for the further improvement of reliability performance in AlGaN/GaN HEMT technology.

Table 1
Reliability performance comparison between vendors A and B

Vendors	I_g (μA) at −10 V	G_{mp} (ms/mm)	I_{max} (mA/mm)
Vendor A before stress	−2.16	260	2065
Vendor A after $T_a = 150$ °C for 48 h	−2.34	−0.07%	−2.30%
Vendor A After $T_a = 150$, 165, 180, 190, 210, and 225 °C (each temperature for 48 h)	−2.14	−57%	−53%
Vendor B before stress	−78.416	263.4	1100
Vendor B after $T_a = 150$ °C for 48 h	−12.564	−32%	−29

5. Conclusion

Elevated temperature lifetesting was performed on 0.25 μm AlGaN/GaN HEMTs grown by MOCVD on 2-in. SiC substrates. The degradation characteristics consist of a decrease of drain current and transconductance, and an increase of channel-on-resistance accompanying by a negligible shift of pinch-off voltage. There is no detectable ohmic metal or gate metal interdiffusion into the epitaxial materials based on FIB/STEM cross-sectional results. The reliability performance was also compared between two vendors of AlGaN/GaN epilayers. The results indicate that the reliability performance of AlGaN/GaN HEMTs could strongly depend on the material quality of AlGaN/GaN epitaxial layers on SiC substrates.

References

[1] Eastman LF. Joint ONR/MURI Review (5/15–16, 2001), CA, USA.
[2] Micovic M, Kurdoghlian A, Janke P, Hashimoto P, Wong DWS, Moon JS, et al. AlGaN/GaN heterostructure field effect transistors grown by nitrogen plasma assisted molecular beam epitaxy. IEEE Trans Electron Dev 2001;48:591–6.
[3] Palmour JW, Sheppard ST, Smith RP, Allen ST, Pribble WL, Smith TJ, et al. Wide bandgap semiconductor devices and MMIC's for RF power applications. In: The Tech Digest Int Electron Dev Meeting. Washington, DC: 2001. p. 17.4.1–4.4.
[4] Mishira UK, Wu YF, Keller BP, Keller S, DenBaars SP. GaN microwave electronics. IEEE Trans Microwave Theory Technol 1998;46:756–61.
[5] Kim H, Tilak V, Green BM, Smart JA, Schaff WJ, Shealy JR, et al. Reliability evaluation of high power AlGaN/GaN HEMTs on SiC substrate. Phys Stat Sol (a) 2001;188: 203–6.
[6] Kim H, Tilak, V, Green BM, Cha, H. Smart JA, Shealy JR, et al. Degradation characteristics of AlGaN/GaN high electron mobility transistors. In: The Tech Digest Int Reliab Phys Symp. Orlando, Florida: 2001. p. 214–8.
[7] Kim H, Tilak V, Thompson RM, Prunty T, Shealy JR, Eastman LF. Hot electron effects on undoped AlGaN/GaN high electron mobility transistors. In: The Tech Digest GaAs Reliab Workshop. Monterey, CA: 2002. p. 5–6.
[8] Hsu SH, Valizadeh P, Pavlidis D, Moon JS, Micovic M, Wong D, et al. Impact of RF stress on dispersion and

power characteristics of AlGaN/GaN HEMTs. The Tech Digest GaAs IC Symp. Monterey, CA: 2000. p. 85–882.

[9] Smorchkova I, Wojtowicz M, Sandhu R, Tsai R, Barsky M, Namba C, et al. Operation in the K-Band and above. IEEE Trans Microwave Theory Tech 2003;51:665–8.

[10] Smorchkova I, Wojtowicz M, Tsai R, Sandhu R, Barsky M, Namba C, et al. AlGaN/GaN HEMTs high power and low noise performance at $f >= 20$ GHz. In: The Tech Digest IEEE Lester Eastman Conf High Perform Dev. 2002. p. 422–7.

[11] Sandhu R, Wojtowicz M, Smorchkova I, Barsky M, Tsai R, Wang J, et al. 3.2 W/mm, 71% PAE AlGaN/GaN HEMT operation at 20 GHz. The Tech Digest Dev Res Conf. 2002. p. 27–8.

[12] Sandhu R, Wojtowicz M, Barsky M, Tsai R, Smorchkova I, Namba C, et al. 1.6 W/mm, 26% PAE AlGaN/GaN HEMT operation at 29 GHz. In: The Tech Digest Int Electron Dev Meeting. Washington, DC: 2001. p. 17.5.1–5.3.

[13] Chou YC, Leung D, Lai R, Grundbacher R, Liu PH, Biedenbender M, et al. On the investigation of gate metal interdiffusion in GaAs HEMTs. In: The Tech Digest GaAs IC Symp. San Diego: 2003. p. 63–6.

[14] Chou YC, Grundbacher R, Leung R, Lai PH, Liu Q, Kan M, et al. Physical identification of gate metal interdiffusion in GaAs PHEMTs. IEEE Electron Dev Lett 2004;25: 64–6.